RAPID COMMUNICATIONS IN MASS SPECTROMETRY
Rapid Commun. Mass Spectrom. **14**, 1654–1661 (2000)

Grazing incidence surface-induced dissociation of protonated peptides generated by matrix-assisted laser desorption/ionization

Andreas Wieghaus[1], Lothar Schmidt[1], Anna M. Popova[2], Viatcheslav V. Komarov[2] and Hartmut Jungclàs[1]*

[1]Department of Chemistry, Philipps-University Marburg, D-35032 Marburg, Germany
[2]Institute of Nuclear Physics, Lomonosov State University, Moscow 119899, Russia

SPONSOR REFEREE: Prof. RG Cooks, Purdue University, USA

The grazing incidence surface-induced dissociation (GI-SID) of various protonated peptides with typical kinetic energies of 350 eV was investigated. Peptide ions were generated by matrix-assisted laser desorption/ ionization (MALDI) using delayed extraction. The collision target surfaces used were aluminum and a liquid film of perfluorinated hydrocarbons. All peptides studied in these experiments showed enhanced fragment ion yields at grazing incidence (GI-SID effect) as observed in our former experiments with other precursor ion types. In general the GI-SID spectra exhibit *N*-terminal a_1-type fragment ions, immonium ions and side-chain fragment ions in the low mass-to-charge region. Fragment ion series of the peptide backbone were not observed, which are typical and abundant in the spectra of established fragmentation techniques like collision-induced dissociation, MALDI post-source decay or surface-induced dissociation at steeper angles. The potential of the GI-SID process to yield useful information for primary structure determination of peptides is indicated by the observed differences in the GI-SID spectra of the isomeric dipeptides LR and IR. Copyright © 2000 John Wiley & Sons, Ltd.

Received 6 July 2000; Accepted 6 July 2000

Tandem mass spectrometry (MS/MS) is a well-established and powerful technique for structure analysis of molecules in the field of peptide sequencing, especially since the development of ionization techniques such as matrix-assisted laser desorption/ionization (MALDI)[1] and electrospray ionization (ESI).[2] In MS/MS, a precursor ion of interest is mass selected, activated, and finally its fragment ions are mass analyzed. Activation and fragmentation have been established so far by gas-phase collisions with inert gases, called collision-induced dissociation (CID), specifically low-energy (eV) and high-energy (keV) CID.[3,4] The mass spectrometric analysis of product ions released by post-source decay (PSD) of precursor ions that have been generated by MALDI (MALDI-PSD) has also evolved into a powerful and sensitive method for structure analysis of biopolymers.[5–7] Surface-induced dissociation (SID), introduced by Cooks and co-workers as an alternative activation technique, is based on low-energy (10–200 eV) collisions of precursor ions with a surface to induce ion dissociation.[8,9] SID experiments have been performed with various devices and ionization methods. Although MALDI is one of the most sensitive ionization methods currently available for biopolymers, SID in combination with a MALDI ion source has only been rarely reported so far.[10,11] Several researchers have demonstrated that SID can lead to extensive and structurally informative fragmentation of peptides.[11–21]

CID, MALDI-PSD, or SID spectra contain a wide range of fragment ion types, i.e. immonium ions $[RCH{=}NH_2]^+$, *N*-terminal fragment ions (*a*-,*b*-,*c*-type ions), *C*-terminal fragment ions (*x*-,*y*-,*z*-type ions), side-chain cleavage ions (*d*-,*v*-,*w*-type ions), and internal fragment ions. (The peptide fragment ion nomenclature used here is based on the conventional scheme proposed by Roepstorff and Fohlmann[22] and modified by Biemann.[3]) However, the types of fragment ions and the extent to which each type is formed vary from method to method.[19,23] For example, in MALDI-PSD the formation of internal ions is rather pronounced in comparison with other methods.[6] Side-chain cleavage ion types observed by low-energy CID, PSD-MALDI, or SID are of lower abundance relative to those detected by high-energy CID.[4,15,24] In general, the fragmentation patterns produced by CID, MALDI-PSD or SID allow unequivocal sequencing of unknown peptides or, at least, it is possible to find partial sequence information which can be used to identify the full amino acid sequence in a database.[7,24] In certain cases, however, the information content of a fragment ion spectrum is not sufficient for unambiguous sequencing. For example, it is difficult or impossible to distinguish isobaric amino acid residues (e.g. the structural isomers leucine and isoleucine), if side-chain cleavage ions required for their differentiation are not observed to a sufficient extent.[25] Since the interpretation of fragmentation spectra is usually the rate-limiting step in sequence determination,[24] any supplementary information, e.g. that obtained from additional fragmentation pathways, can enhance the determination procedure by reducing the number of possible sequences to be considered.

SID experiments are usually performed at steep angles of incidence (typically 45°). In a few cases, often because of

*Correspondence to: H. Jungclàs, Department of Chemistry, Phillips-University Marburg, D-35032 Marburg, Germany.
E-mail: jungclas@mailer.uni-marburg.de
Contract/grant sponsor: Deutsche Forschungsgemeinschaft, Bonn.
Contract/grant sponsor: NATO, Brussels.

experimental necessities given, SID experiments have been arranged in which the precursor ions undergo grazing or nearly grazing collisions with the surface.[14,15,26–30] In some devices in which shallow collision angles were employed, a smaller internal energy uptake of the precursor ions was observed in comparison with conventional SID instruments.[15,28]

In our laboratory, ion/surface collision experiments in the collision energy regime of several 100 eV have shown the effect of enhanced surface-induced dissociation at grazing incidence for various polyatomic ions.[31,32] From the hitherto existing experimental results it is reasonable to conclude that the excitation mechanism involved in grazing incidence SID (GI-SID) is different from that in normal SID. A quantum mechanical model of the GI-SID process has been developed, in which polyatomic molecules with substructures consisting of chains of biatomic dipole groups are sliding along a regular matrix of surface atoms.[33–35] Because of the interaction with the periodic Coulomb field of the surface, several independent collective vibrational states (excimols) are induced in these chains. An analytical expression for the probability to gather a certain number of excimols in a molecule has been derived in a previous study.[35] This probability depends on the number of dipole groups available in chain-like substructures of the precursor molecule and on the probability P_{01} of excitation of one excimol. The probability P_{01} strongly depends on the velocity of the grazing precursor ion, since the excitation of excimols induced by interaction with the periodic Coulomb field of the surface is a resonant process. The accumulated energy of several excimols is transferred by dipole/dipole interactions to a trap-bond which is cleaved if the transferred energy exceeds a specific threshold value.[33–35]

By virtue of the very special choice of precursor ion types in previous GI-SID experiments (e.g. cesium-attached cyclodextrin derivatives,[31] hexadecylpyridinium and verapamil ions[32]), it was difficult to compare the GI-SID spectra with those of the established fragmentation techniques. Thus, in the present work, GI-SID of protonated peptides generated by MALDI has been studied to make such comparisons possible. The experiments were not intended to check the excimol theory. Rather, the main aim of this investigation was to find out whether the GI-SID effect is also observed for peptide ions and, if possible, to determine the fragment ion types and the extent to which they are formed. The results should allow assessment of the potential of GI-SID spectra to yield information which could be helpful in sequence determination of peptides.

EXPERIMENTAL

Instrumentation

The experiments were carried out on our modified home-built ^{252}Cf plasma desorption time-of-flight (TOF) mass spectrometer which has been employed previously for GI-SID experiments.[31,32,35] Several modifications were made to enable precursor ion production by matrix-assisted laser desorption/ionization with delayed ion extraction. The present instrument configuration is schematically shown in Fig. 1. The pressure in the mass spectrometer was $\approx 1 \times 10^{-6}$ Torr. A nitrogen laser (model VSL-335ND-S, Laser Science, Franklin, MA, USA) was used for ion desorption. The laser beam was attenuated by means of a circular variable neutral density filter and focused with a quartz lens of 100 mm focal length onto the sample at

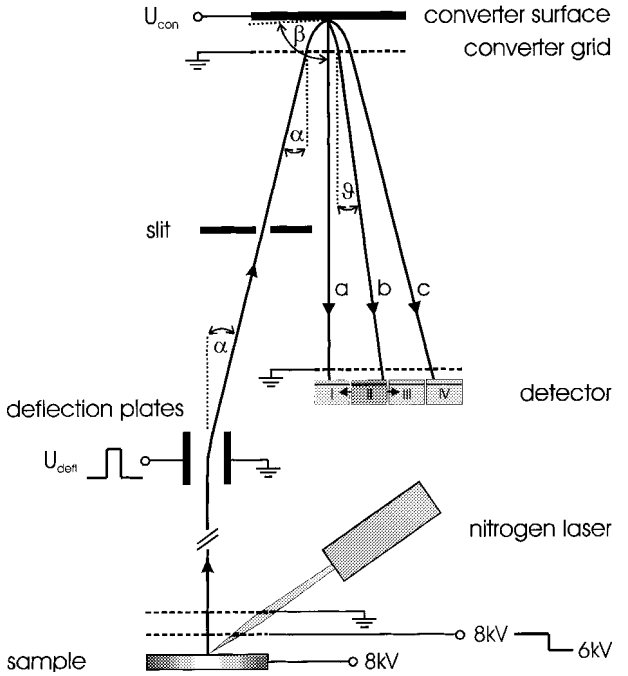

Figure 1. Schematic of the MALDI/GI-SID experiment. The three labeled trajectories correspond to (a) sputtered ions, (b) to a special GI-SID fragment ion and (c) to intact reflected precursor ions. Four different detector positions were used (I–IV). For ion detection see text for further explanations.

about 45°. All experiments were performed at threshold laser irradiance. Desorbed ions were extracted in a dual-stage acceleration region with time-delayed, pulsed ion extraction using two high-voltage power supplies, a delay generator and a fast high-voltage transistor switch (model HTS 50-06, Behlke Electronic, Kronberg, Germany). Positive ions leaving the ion source with a kinetic energy of about 8 keV were deflected by a pair of deflection plates, passed through a slit and reached a converter grid under a deflection angle $\alpha \approx 12°$. For the definition of the different angles, see Fig. 1. Mass selection of desired precursor ions, i.e. protonated peptides in these experiments, was arranged by pulsing the deflection voltage U_{defl} using a digital delay/pulse generator (model DG135, Stanford Research Systems, Sunnyvale, CA, USA) and a fast high-voltage push-pull switching unit (model GHTS 30, Behlke Electronic).

The converter consists of a converter foil at the potential U_{con}, which serves as target for the collision experiments, and a grounded grid mounted parallel to the converter surface at a distance of 7 mm. For $U_{\mathrm{con}} < 0$ the converter is operated in an ion-to-electron conversion mode resulting in post-acceleration of the precursor ions in the converter field and acceleration and detection of secondary electrons arising from ion/surface collisions. Operating the converter in the ion-to-electron conversion mode allows the setup to be used to take normal MALDI-TOF mass spectra with a typical mass resolution of $m/\Delta m \geq 1000$.

For $U_{\mathrm{con}} > 0$ the mass selected precursor ions hit the converter surface with a collision energy

$$E_{\mathrm{c}} = e \cdot (U_{\mathrm{acc}} - U_{\mathrm{con}})$$

under an incidence angle β (to the surface normal), which is

given by

$$\cot^2 \beta = \cot^2 \alpha - \frac{U_{con}}{U_{acc} \sin^2 \alpha}$$

and takes values in the interval [α,90 °]. In the special case

$$U_{con} = U_{gi} = U_{acc} \cos^2 \alpha$$

the precursor ions undergo grazing collisions with the converter surface ($\beta = 90°$). Indeed, by virtue of setup modifications (e.g. changing the converter surface), U_{gi} was changed over a moderate range within this study, but the typical value was $U_{gi} = 7650$ V resulting in a 'collision' energy of 350 eV. For $0 \text{ V} < U_{con} \leq U_{gi}$ secondary cations resulting from ion/surface collisions are accelerated by the converter potential. Secondary cations which are sputtered from the surface leave the converter grid under an 'outcome' angle $\vartheta_a = 0°$, i.e. perpendicular to the surface (trajectory a in Fig. 1). Secondary cations resulting from SID fragmentation of precursor ions leave the converter under an angle ϑ_b (trajectory b in Fig. 1), where ϑ_b depends mainly on the ratio m_f/m_p of the SID fragment ion's mass m_f and the precursor ion's mass m_p. The angle ϑ_b takes values in the interval [0, α]. For U_{con} close to or above U_{gi} intact scattered or reflected precursor ions leave the converter under an angle $\vartheta_c \approx \alpha$ (trajectory c in Fig. 1).

Fragment ions (m_{mf}) resulting from metastable decay of precursor ions after passing the deflection plates are reflected in the converter field, if

$$U_{con} \geq \frac{m_{mf}}{m_p} \cdot U_{gi}.$$

Since peaks of these metastable fragment ions appear in the spectra for $U_{con} < U_{gi}$ and remain constant for rising converter potentials, they can unequivocally be identified and distinguished from GI-SID fragment ions. In addition, because of the small distance between the converter grid and the converter surface (7 mm), metastable fragment ions reach the detector nearly at the same time as intact reflected precursor ions and thus do not interfere with the GI-SID fragment ion peaks in the spectra.

After passing through a secondary flight path of 0.93 m the secondary ions were detected by a hybrid detector composed of a microchannel plate (model F4293-07, Hamamatsu, Japan) and a mesh type secondary electron multiplier (model R2362, Hamamatsu). The front side of the microchannel plate was at −3.8 kV resulting in post-acceleration of positive ions. In front of the detector a slit stop was assembled to produce a rectangular (17×10) mm^2 active detector area. By means of a linear vacuum feedthrough the detector could be moved horizontally over a distance of 51 mm. Thus, by using four different detector positions (I–IV), a total area of (68×10) mm^2 could be covered, which was sufficient to detect all possible kinds of ions leaving the converter, i.e. sputtered ions, fragment ions and intact reflected precursor ions.

The transient signal output of the detector was digitized by a digital sampling oscilloscope (model 54510B, Hewlett-Packard, Palo Alto, CA, USA) using a time resolution of 2 ns/channel. The time-of-flight data were transferred to a PC after each shot for averaging, storage and analysis.

Collision surfaces

Stretched aluminized polyester foils, without further treatment or covered by a thin liquid film of perfluorinated hydrocarbons, were used as collision surfaces. For the preparation of the film of perfluorinated hydrocarbons the nonvolatile liquid constituents of a perfluorinated paste (trade name Triboflon III, obtained from Merkel, Hamburg, Germany) were extracted by a volatile liquid perfluorinated oil and spread over the aluminized foil. Under the given vacuum conditions bare aluminum foils were inevitably covered with hydrogen adsorbates (pump oil), whereas the perfluorinated surface could be expected to remain clean from hydrocarbon impurities.[36,37]

Materials and sample preparation for precursor ions

For all peptide samples α-cyano-4-hydroxycinnamic acid (10 g L^{-1} in acetone) was used as matrix. Peptides were dissolved in an aqueous 0.1% trifluoroacetic acid solution (1 g L^{-1}). Analyte and matrix solutions were mixed in order to get molar analyte-matrix ratios within the range of 1:300 (e.g. for PR) to 1:1500 (e.g. for substance P). 100 μL of the mixture were sprayed on a polished stainless steel target by a nebulizer.[38] The resulting homogeneously coated targets were washed with water to remove salts and other impurities. Dipeptides were purchased from Bachem Biochemica (Heidelberg, Germany); all other peptides and α-cyano-4-hydroxycinnamic acid were from Sigma Chemical (St. Louis, MO, USA).

For PEG 1000 (Fluka, Buchs, Switzerland), dithranol (Aldrich, Steinheim, Germany) was used as matrix and sodium trifluoroacetate (Fluka) as cation supplier at a molar ratio of analyte/salt/matrix = 1:1:500.

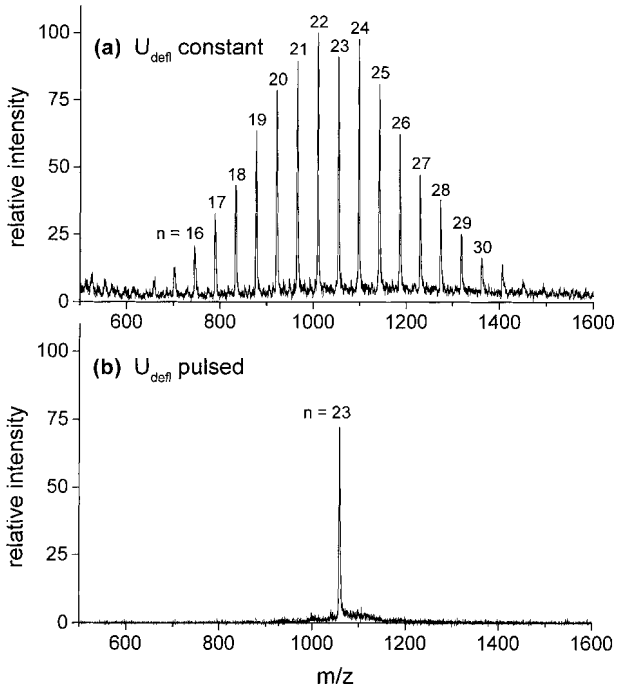

Figure 2. Performance of the mass selection method using a pulsed deflection voltage U_{defl} exemplified by sodium-attached PEG oligomers from PEG 1000. The oligomer (n = 23) at mass 1053.6 u was selected without significant intensity loss, whereas the neighboring signals at ± 44 u were completely suppressed. In this experiment the converter was operated in the ion-to-electron conversion mode. Both spectra were averaged over 100 single-shot spectra.

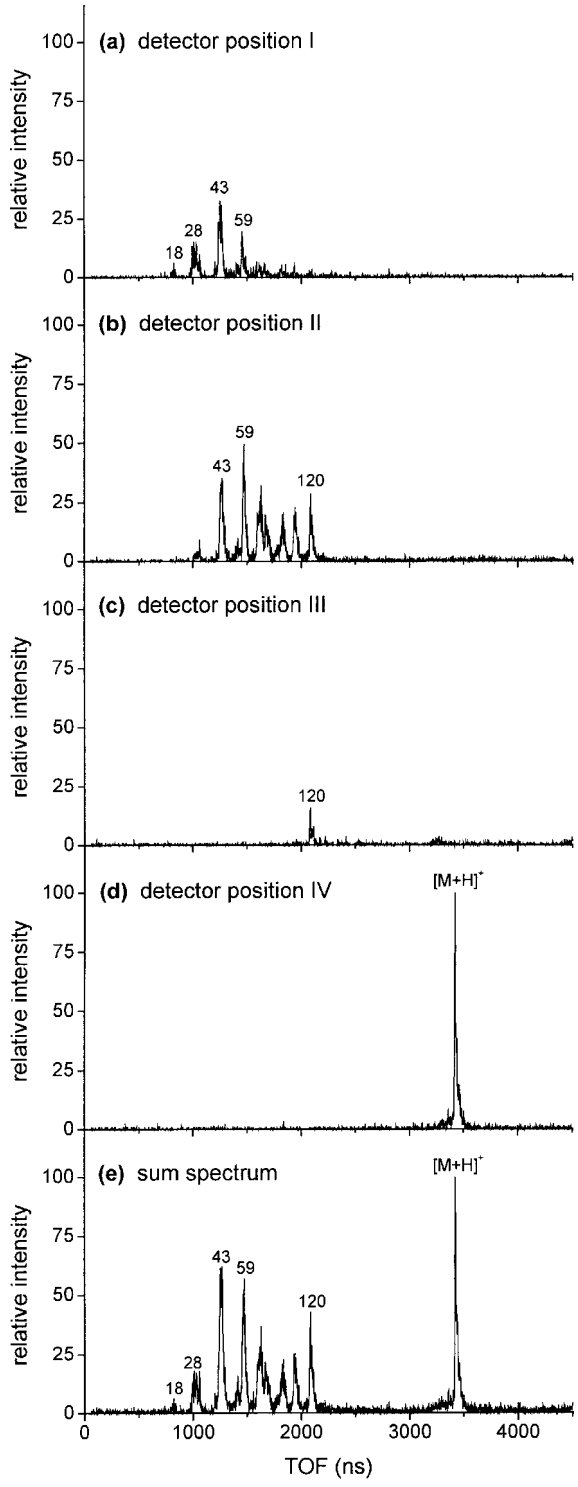

Figure 3. Single GI-SID spectra taken at different detector positions (panels a–d) and the resulting summed GI-SID spectrum (panel e) of the protonated dipeptide FR. The further the detector was moved outwards, the larger the fragment ions detected. This observation can be easily explained, since fragment ions have inherited the precursor ion velocity component perpendicular to the converter field direction. At detector position IV (panel d) even intact reflected precursor ions were detected. The collision surface used here was aluminum.

Measurement protocol and mass calibration

In Fig. 2 the performance of the mass selection method using a pulsed deflection voltage U_{defl} is exemplified by polyethylene glycol (PEG) 1000.

Because of the limited detector area a GI-SID spectrum of mass selected precursor ions, i.e. protonated peptides in this work, had to be composed of four single spectra, each taken for $U_{con} = U_{gi}$, but at different detector positions (marked by I, II, III and IV in Fig. 1). Each single spectrum itself was averaged over several (typically 50) laser shots. Figure 3 displays these four single spectra and their resulting sum spectrum for the protonated dipeptide FR.

For mass calibration of each GI-SID spectrum one additional spectrum was taken for $U_{con} = -4.5$ kV (ion-to-electron conversion mode). From the arrival time of the secondary electrons the time t_0 could be calculated at which the precursor ions arrive at the collision surface for $U_{con} = U_{gi}$. As the arrival time t_p of the intact reflected precursor ions at the detector for $U_{con} = U_{gi}$ was known from the GI-SID spectrum, a calibration factor A could be calculated by

$$A = \frac{t_p - t_0}{\sqrt{m_p}}$$

and the mass calibration of the GI-SID time-of-flight spectrum ($t_0 \leq t \leq t_p$) was given by

$$m/z = \left(\frac{t - t_0}{A}\right)^2.$$

The mass resolution of a GI-SID spectrum is mainly affected by the time spread of the precursor ion signal. Thus the mass resolution of the GI-SID spectra decreases with increasing mass of the precursor ions.

RESULTS AND DISCUSSION

GI-SID effect

The GI-SID phenomenon is exemplified in Fig. 4 by results of collision experiments with protonated molecules of RPPGFSP (bradykinin fragment 1–7) using a liquid film of perfluorinated hydrocarbons as collision surface. The incidence angle β is plotted as a function of the converter potential U_{con} (Fig. 4(a)). At an incidence angle $\beta = 90°$ (i.e. $U_{con} = U_{gi}$), grazing collisions of the peptide ions with the surface are realized. The yield of secondary ions resulting from ion/surface collisions is also shown as a function of U_{con} (Fig. 4(b)). The secondary ion yield was measured at the detector positions I and II, at which sputter ions and SID fragment ions were detected, whereas metastable fragment ions and intact scattered or reflected precursor ions were not detected. The mean values and standard deviations given here were obtained by averaging the secondary ion yield over 22 laser shots for each value of U_{con}. In order to eliminate the influence of sample inhomogeneity, 22 laser shots were successively fired on an initially fresh sample spot, and after each laser pulse the secondary ion yield was determined and the value of U_{con} was changed before firing the next laser pulse. This procedure was repeated for 21 further sample spots, for which each series of measurements was started with a different value of U_{con}.

At low converter potentials and thus at steep incidence angles of the precursor ions, the secondary ion spectra consisted of ions which were sputtered from the perfluorinated surface, i.e. $[CF]^+$, $[CF_3]^+$, $[C_2F_4]^+$ and $[C_3F_7]^+$ (Fig. 4(c)). Additionally, protons were generated in ion/surface collisions at steep incidence angles. The conclusion that these protons were not sputtered ions but SID fragment ions

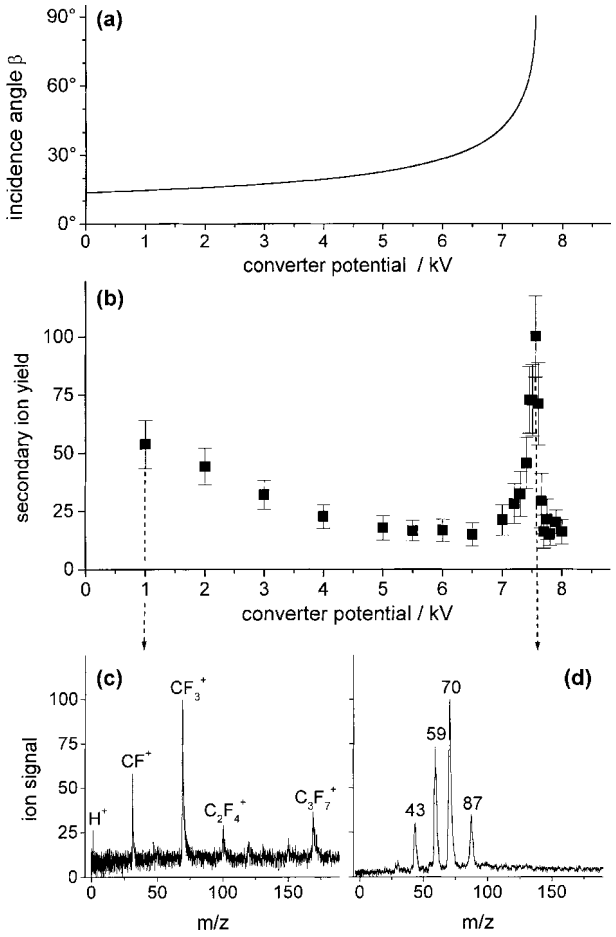

Figure 4. The GI-SID phenomenon exemplified by results of ion/surface collision experiments using protonated RPPGFSP as the precursor ion and a liquid film of perfluorinated hydrocarbons as collision surface. The incidence angle β (measured to the surface normal), at which the precursor ions impinge on the surface (a) and the overall yield of secondary cations (b) are given as functions of the converter potential U_{con}. The secondary ion spectra at low converter potentials and thus at steep incidence exhibit ions which were sputtered from the perfluorinated surface (c). The significant maximum of the secondary ion yield at grazing incidence ($\beta = 90°$) was caused by fragment ions in the low mass-to-charge region (spectrum d).

was discussed in a recent paper.[32] With increasing converter potentials and thus increasing incidence angles β, the yield of sputter ions decreased, whereas the yield of SID fragment ions increased drastically close to U_{gi} resulting in a sharp and intense maximum at grazing incidence (Fig 4(b)). The mass spectrum of the GI-SID fragment ions causing this maximum is shown in Fig. 4(d) and will be discussed later in connection with Fig. 6. Analogous curves of the secondary ion yield – with a pronounced maximum at grazing incidence – were observed for all peptide ions studied. Thus the steep increase in the fragment ion yield close to the grazing incidence condition (GI-SID effect), observed before in experiments with various kinds of precursor ions,[31,32] also occurs for peptide ions. Converter potentials at which GI-SID ions were observed covered a range of about 150 V (FWHM), which is assumed to be caused mainly by the divergence of the precursor ion beam. Of course a variation in U_{con} also caused a change in the collision energy E_c. But one has to take into consideration that close to U_{gi} a small increase in U_{con} and thus a small decrease in E_c (linear to U_{con}) leads to a large nonlinear increase in the incidence angle β (Fig 4(a)). Additionally, in previous experiments, the GI-SID phenomenon was observed for a wide range of grazing incidence collision energies E_c.[34,35] Thus, in the first place, the GI-SID effect is an effect of the incidence angle β. Nevertheless, the 'collision' energy E_c at grazing incidence influences the yield of GI-SID fragment ions, since the GI-SID fragmentation probability depends on the velocity of the precursor ions which slide along the surface.[34,35]

GI-SID spectra of dipeptides

In an initial set of experiments, GI-SID spectra of various dipeptides were taken, since their interpretation was expected to be more straightforward than those of larger peptides. Figure 5 shows the GI-SID spectra of the protonated dipeptides RR, PR, FR and YR using aluminum as collision surface. The GI-SID spectrum of RR in Fig. 5(a) exhibits peaks at *m/z* 43, 44, 59, 70, 73 and 87. In the GI-SID spectrum of PR (Fig. 5(b)), the peak at *m/z* 70 is much more pronounced in comparison with that of RR. This increase is obviously caused by *N*-terminal a_1-fragment ions corresponding to immonium ions of proline. The GI-SID spectrum of FR (Fig. 5(c)) yields additional peaks at *m/z* 77, 91, 104 and 120. The latter peak released by *N*-terminal a_1-fragmentation corresponds to immonium ions of phenylalanine, whereas the other peaks are caused by side-chain fragmentation. In the GI-SID spectrum of YR (Fig. 5(d)), the fragment ion peaks at *m/z* 107, 119 and 136 were produced by side-chain fragmentation and *N*-terminal a_1-fragment ions (immonium ions of tyrosine), respectively. The side-chain fragments of both phenylalanine and tyrosine can be understood easily by the structure of the respective amino acid residue. The typical fragmentation pattern produced by arginine (*m/z* 59, 70, 73 and 87) was observed in the GI-SID spectra of all arginine-containing dipeptides studied in this work. Presumably, they were observed at high abundances because of the ability of arginine to stabilize positive charge at a number of different sites, but it is unclear whether they were formed by fragmentation of immonium ions or by alternative pathways.[39,40] In this regard it may be noteworthy that immonium ions of arginine (*m/z* 129) were not observed in the GI-SID spectra of arginine-containing dipeptides. GI-SID experiments with other dipeptides (GR, HR, IR and LR) yielded analogous results.

Immonium ions did not exclusively arise as *N*-terminal a_1-ions in the GI-SID process. For example, the GI-SID spectrum of RF (not shown here) also exhibits immonium ions of phenylalanine at *m/z* 120. Nevertheless, they were observed at a lower relative abundance in comparison to those in GI-SID of FR.

The observed GI-SID fragment ions are known in part from other fragmentation methods, too. For example, the fragments *m/z* 59, 70, 73 and 87 appear also in high-energy CID spectra of arginine-containing peptides,[39,40] *m/z* 70 and 87 occur as arginine-related fragment ions in MALDI-PSD spectra also.[7] But it is important to note that the GI-SID process also yields additional fragment ion types relative to established fragmentation techniques. For example, the side-chain fragment ions of phenylalanine (*m/z* 77, 91, 104) and tyrosine (*m/z* 107, 119) occur at significantly lower relative abundances or not at all in high-energy CID[39] or MALDI-PSD spectra. However, such comparisons of

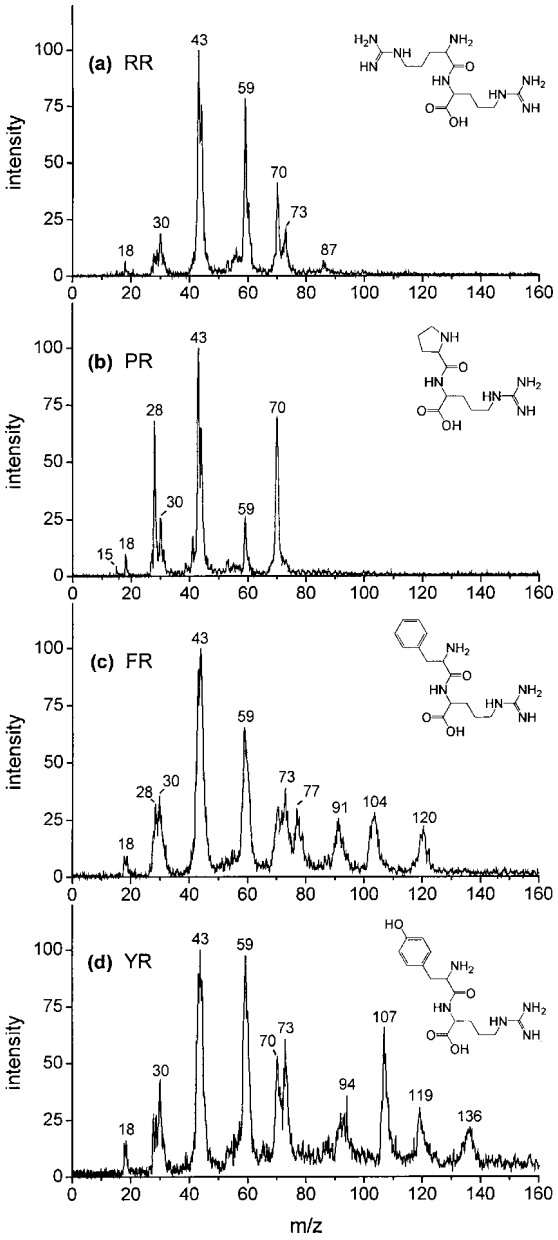

Figure 5. GI-SID spectra of the protonated dipeptides RR, PR, FR, and YR. The collision surface used here was aluminum.

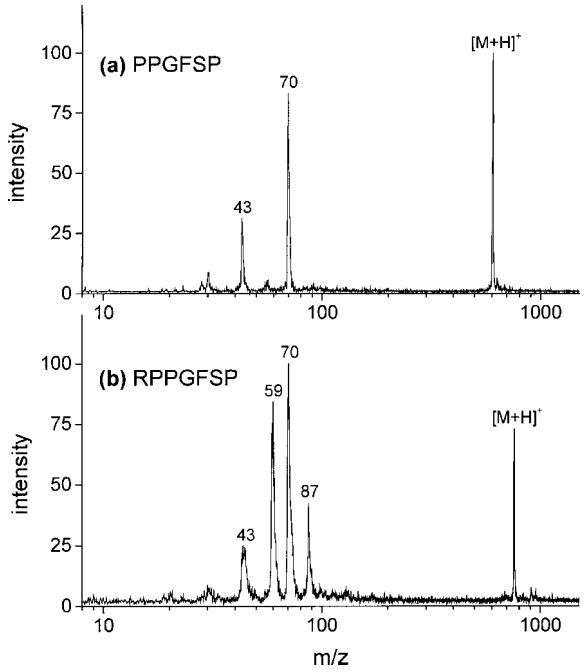

Figure 6. GI-SID spectra of protonated PPGFSP (bradykinin fragment 2–7) and protonated RPPGFSP (bradykinin fragment 1–7) using a liquid film of perfluorinated hydrocarbons as collision surface. Note the logarithmic scale of the *m/z*-axis.

spectra obtained by different instrument types have to be interpreted with caution, since relative abundances in fragmentation spectra can be influenced by experimental conditions, especially by discrimination against fragment ions in the low mass-to-charge region.

GI-SID spectra of oligopeptides

In further experiments larger peptides were considered. Figure 6 shows the GI-SID spectra of PPGFSP (bradykinin fragment 2–7) and RPPGFSP (bradykinin fragment 1–7). The GI-SID spectrum of PPGFSP is dominated by a peak at *m/z* 70, presumably caused by *N*-terminal a_1-fragment ions corresponding to immonium ions of proline. The GI-SID spectrum of RPPGFSP exhibits additional peaks at *m/z* 59 and 87, obviously caused by fragment ions of the arginine residue added on the *N*-terminal side. Whereas the fragment ions at *m/z* 43 were expected to correspond also to side-chain fragment ions of arginine and thus their appearance in the GI-SID spectrum of RPPGFSP could be explained, their origin in the GI-SID spectrum of the arginine-free PPGFSP is not understood.

Apart from these fragment ions in the low mass-to-charge region, no additional fragment ions were observed, in particular no *N*-terminal fragment ions (*a*-, *b*-, *c*-, and *d*-type ions), *C*-terminal fragment ions (*x*-, *y*-, *z*-type ions) or internal fragment ions, which are all typical and abundant exponents in fragmentation spectra of established MS/MS methods such as CID, MALDI-PSD or normal SID. This observation is also valid for further peptides studied in this work, e.g. RRR, RRRR, YGGFL (leucine enkephalin), RPPGFSPFR (bradykinin), or RPKPQQFFGLM-NH_2 (substance P). For example, the GI-SID spectrum of leucine enkephalin (shown in Fig. 7) is dominated by immonium ions (*m/z* 136) and side-chain fragment ions (*m/z* 107) of tyrosine, and immonium ions of phenylalanine (*m/z* 120).

GI-SID spectra of the isomeric peptides LR and IR

The differentiation of isobaric amino acid residues is generally difficult or impossible in peptide sequencing by tandem mass spectrometry due to the dominance of fragment ion series of the peptide backbone. For this purpose, the observation of side-chain specific fragment ions (mostly *d*- or *w*-type ions) has proven to be crucial.[25] In this regard, the comparison of the GI-SID spectra of the isomeric peptides LR and IR given in Fig. 8 may be interesting. The GI-SID spectrum of IR exhibits a clear peak at *m/z* 57 which is not present in the GI-SID spectrum of LR. The additional appearance of this peak in the GI-SID spectrum of IR is obviously due to fragment ions resulting from dissociation of the C^{α}-C^{β} bond (backbone carbon designated α) of the isoleucine side chain in contrast to the

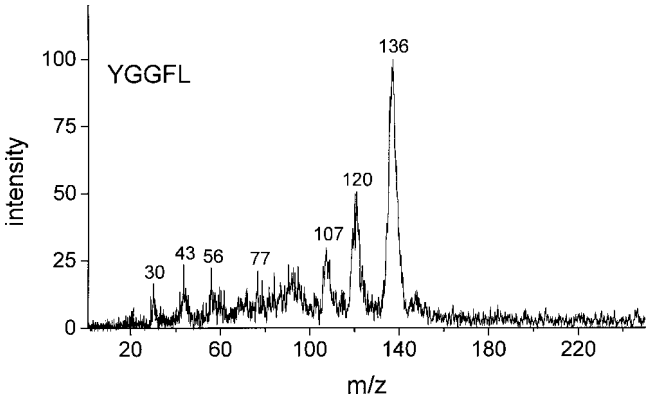

Figure 7. GI-SID spectrum of protonated YGGFL (leucine enkephalin) using aluminum as collision target surface.

favored dissociation of the C^{β}-C^{γ} bond of the leucine side chain.

To our knowledge, this fragmentation pathway of isoleucine residues has not been reported for other fragmentation methods. The observed reproducible difference in their GI-SID spectra allows one to distinguish between the isomeric peptides LR and IR. This result may be conceived as a hint that the GI-SID process yields additional fragment ion types in the low mass-to-charge region, which may be helpful in the primary structure analysis of peptides. Of course, this conclusion is preliminary, since only dipeptides were investigated in this experiment.

Conversion efficiency

The conversion efficiency of a SID process is defined as the sum of fragment ion abundances divided by the total primary ion abundance. The values measured in different SID instruments employing various precursor ions and surfaces fall in a wide range from 1 to 66 %.[9,19,27,41] In previous GI-SID experiments using hexadecylpyridinium and verapamil ions generated by fission fragment desorption as precursor ions and a liquid film of perfluorinated hydrocarbons as collision surface, conversion efficiencies of 40–70% were measured.[32] It was difficult to obtain absolute values of the conversion efficiency in the MALDI/GI-SID instrument used in this work. Nevertheless, the GI-SID fragment ion intensity I_f obtained for $U_{con} = U_{gi}$ relative to the primary ion intensity I_p obtained for $U_{con} = -4500$ V (ratio I_f/I_p) yields a rough estimation of the GI-SID conversion efficiency, which allows one to compare the conversion efficiencies of different peptide ions. First experiments employing this procedure with various dipeptide precursor ions and aluminum as collision surface yielded values of I_f/I_p ranging from (24 ± 4) % for PR to (49 ± 11) % for RR. The mean values and standard deviations given here were obtained by averaging over several laser shots (typical 16, for I_p and 30 for I_f) each fired on a different spot of the sample.

CONCLUSIONS

In the experimental setup described here matrix-assisted laser desorption/ionization has been combined for the first time with surface-induced dissociation (SID) to study the grazing incidence SID (GI-SID) of protonated peptides with

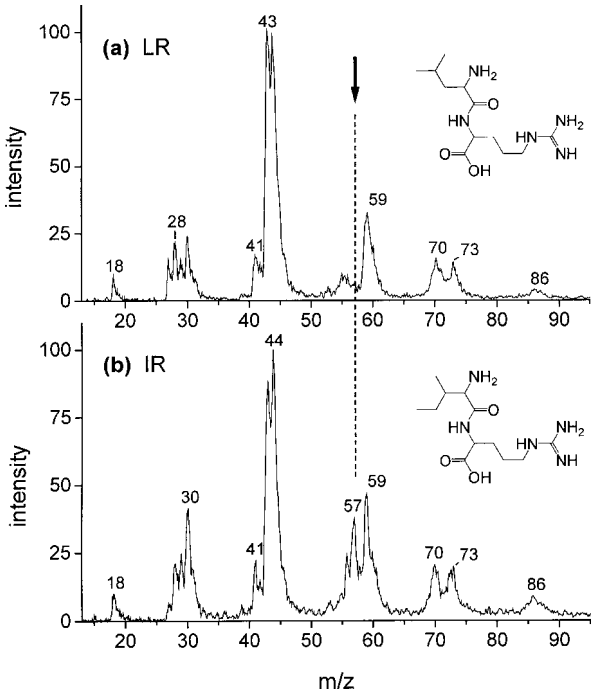

Figure 8. Comparison of the GI-SID spectra of the isomeric protonated dipeptides LR and IR using aluminum as collision surface.

kinetic energies of 350 eV. The results obtained in this work show that the GI-SID effect, i.e. the strongly enhanced fragmentation yield at grazing incidence, also occurs for peptide ions. The GI-SID spectra of peptides are dominated by *N*-terminal a_1-type fragment ions, immonium ions and side-chain fragment ions in the low mass-to-charge region. Apart from a_1-type ions, backbone fragment ions were not observed.

The observation that only small fragment ions appear in the GI-SID spectra leads to the conclusion that the GI-SID fragmentation of a precursor ion M^+ either results exclusively in small charged fragments Fr^+ and corresponding large neutral fragments of type [M-Fr], or the precursor ion undergoes multiple bond cleavages preventing the formation of large fragment ions. In the frame of the GI-SID model the latter is more probable. The GI-SID model is based on resonant excimol excitation of identical dipole groups in substructures of the molecule. In the case of peptide molecules such substructures are present in the side chains. Because of the resonant behavior of the excimol excitation process, a maximum uptake of internal energy is expected for a velocity range, which depends on the excimol energy and on surface Coulomb parameters. The velocities of the grazing peptide precursor ions employed in this work are close to this resonant velocity range resulting in a high-energy accumulation and likely to multiple bond cleavages. For velocities far from the resonant velocity a lower uptake of internal energy is expected, possibly with the consequence that high mass fragment ions are also generated.

GI-SID spectra of the isomeric peptides LR and IR show that it is possible to distinguish between leucine and isoleucine by means of their different GI-SID fragment ions in the low mass region, indicating that GI-SID may yield additional fragmentation pathways and thus additional information, which could facilitate peptide sequence determination in certain cases. Further studies will be

performed to improve our understanding of the GI-SID process and with it knowledge of fragmentation mechanisms of polyatomic molecules, in particular of peptide ions.

In the future, we also intend to enhance the performance of our MALDI/GI-SID device, especially the mass resolution of the GI-SID spectra. In this regard the application of a collision device using delayed extraction to improve the resolving power for ion/surface collision products, as proposed in a recent paper,[42] seems to be a promising starting point.

Acknowledgements

This work was financially supported by the Deutsche Forschungsgemeinschaft (Bonn) and NATO (Brussels) which is gratefully acknowledged. The authors would like to thank M. Wehofsky and R. Hoffmann (Biologisch-Medizinisches Forschungszentrum, University of Duesseldorf) for measuring MALDI-PSD reference spectra.

REFERENCES

1. Karas M, Bachmann D, Bahr U, Hillenkamp F. *Int. J. Mass Spectrom. Ion Processes* 1987; **78**: 53.
2. Fenn JB, Mann M, Meng CK, Wong SF, Whitehouse CM. *Science* 1989; **246**: 64.
3. Biemann K. *Biomed. Environ. Mass Spectrom.* 1988; **16**: 99.
4. Medzihradszky KF, Maltby DA, Qiu Y, Hall SC, Chen Y, Burlingame AL. *Int. J. Mass Spectrom. Ion Processes* 1997; **160**: 357.
5. Spengler B, Kirsch D, Kaufmann R, Jaeger E. *Rapid Commun. Mass Spectrom.* 1992; **6**: 105.
6. Spengler B. *J. Mass Spectrom.* 1997; **32**: 1019.
7. Chaurand P, Luetzenkirchen F, Spengler B. *J. Am. Soc. Mass Spectrom.* 1999; **10**: 91.
8. Mabud MdA, Dekrey MJ, Cooks RG. *Int. J. Mass Spectrom. Ion Processes* 1985; **67**: 285.
9. Cooks RG, Ast T, Mabud MdA. *Int. J. Mass Spectrom. Ion Processes* 1990; **100**: 209.
10. Wieghaus A, Schmidt L, Popova AM, Komarov VV, Jungclas H. *32th Annual Conference of the Deutsche Gesellschaft für Massenspektrometrie*, Oldenburg, Germany, 1999.
11. Riederer DE, Haney LL, Hilgenbrick AR, Beck JR. *48th ASMS Conference on Mass Spectrometry and Allied Topics*, Long Beach, CA, 2000.
12. Cooks R, Amy J, Bier M, Schwartz J, Schey K. *Adv. Mass Spectrom.* 1989; **11**: 33.
13. Williams ER, Henry KD, McLafferty FW, Shabanowitz J, Hunt DF. *J. Am. Soc. Mass Spectrom.* 1990; **1**: 413.
14. Aberth W. *Anal. Chem.* 1990; **62**: 609.
15. Despeyroux D, Wright AD, Jennings KR. *Int. J. Mass Spectrom. Ion Processes* 1993; **126**: 95.
16. Cole RB, LeMeillour S, Tabet JC. *Anal. Chem.* 1992; **64**: 365.
17. McCormack AL, Somogyi Á, Dongré AR, Wysocki VH. *Anal. Chem.* 1993; **65**: 2859.
18. Chorush RA, Little DP, Beu SC, Wood TD, McLafferty FW. *Anal. Chem.* 1995; **67**: 1042.
19. Dongré AR, Somogyi Á, Wysocki VH. *J. Mass Spectrom.* 1996; **31**: 339.
20. Gu C, Somogyi Á, Wysocki VH, Medzihradszky KF. *Anal. Chim. Acta* 1999; **397**: 247.
21. Tsaprailis G, Somogyi Á, Nikolaev EN, Wysocki VH. *Int. J. Mass Spectrom.* 2000; **195/196**: 467.
22. Roepstorff P, Fohlmann J. *Biomed. Mass Spectrom.* 1984; **11**: 601.
23. Rouse JC, Yu W, Martin SA. *J. Am. Soc. Mass Spectrom.* 1995; **6**: 822.
24. Yates JR III, Eng JK, Clauser KR, Burlingame AL. *J. Am. Soc. Mass Spectrom.* 1996; **7**: 1089.
25. Johnson RS, Martin SA, Biemann K, Stults JT, Watson JT. *Anal. Chem.* 1987; **59**: 2621.
26. Cooks RG, Ast T, Beynon JH. *Int. J. Mass Spectrom. Ion Phys.* 1975; **16**: 348.
27. Ijames CF, Wilkins CL. *Anal. Chem.* 1990; **62**: 1295.
28. Castoro JA, Nuwaysir LM, Ijames CF, Wilkins CL. *Anal. Chem.* 1992; **64**: 2238.
29. Snowdon KJ, Golichowski AP, Harder R, Nesbitt A. *Int. J. Mass Spectrom. Ion Processes* 1998; **174**: 73.
30. Krischok S, Mueller H, Kempter V. *Nucl. Instrum. Methods Phys. Res. Sect. B* 1999; **157**: 198.
31. Schmidt L, Fritsch HW, Jungclas H. *Rapid Commun. Mass Spectrom.* 1993; **7**: 507.
32. Wieghaus A, Schmidt L, Popova AM, Komarov VV, Jungclas H. *J. Mass Spectrom.* 1999; **34**: 1178.
33. Schmidt L, Komarov VV, Popova AM, Jungclas H. *Nucl. Instrum. Methods Phys. Res. Sect. B* 1997; **122**: 224.
34. Komarov VV, Popova AM, Schmidt L, Jungclas H. *Mol. Phys.* 1997; **91**: 139.
35. Jungclas H, Wieghaus A, Schmidt L, Popova AM, Komarov VV. *J. Am. Soc. Mass Spectrom.* 1999; **10**: 471.
36. Pradeep T, Miller SA, Cooks RG. *J. Am. Soc. Mass Spectrom.* 1993; **4**: 769.
37. de Maaijer-Gielbert J, Beijersbergen JHM, Kistemaker PG, Weeding TL. *Int. J. Mass Spectrom. Ion Processes* 1996; **153**: 119.
38. Tuszynski W, Angermann R, Metzger JO, Woisch R. *Nucl. Instrum. Methods Phys. Res. Sect. B* 1994; **88**: 184.
39. Falick AM, Hines WM, Medzihradszky KF, Baldwin MA, Gibson BW. *J. Am. Soc. Mass Spectrom.* 1993; **4**: 882.
40. Madden T, Welham KJ, Baldwin MA. *Org. Mass Spectrom.* 1991; **26**: 443.
41. Somogyi Á, Kane TE, Ding JM, Wysocki VH. *J. Am. Chem. Soc.* 1993; **115**: 5275.
42. Haney LL, Riederer DE. *Anal. Chim. Acta* 1999; **397**: 225.

